ICNC 2019 - 11th International conference on Nuclear Criticality Safety
September 15-20, 2019 – Paris, France

SAND2019-6380C

PARAMETRIC ANALYSIS OF HANDBOOK METAL-WATER CRITICAL MASS CURVES WITH MCNP

William M. Cook [(1)*], John A. Miller [(1)], Shawn Henderson [(1)], Jennifer Alwin [(2)], Forrest Brown [(2)]

[(1)]Sandia National Laboratories, 1515 Eubank Blvd SE; MS# 1141; Albuquerque, NM 87123; USA
[(2)]Los Alamos National Laboratory, P.O. Box 1663; Las Alamos, NM 87545; USA
** wmcook@sandia.gov*

ABSTRACT

The purpose of this paper is to present and discuss the methodology, results, and conclusions of an analysis of spherical, homogenous metal-water mixtures in MCNP-6.2 with ENDF/B-VII.1 data. The parametric analysis reproduced curves of critical fissile mass as a function of metal-water mixture density (i.e., concentration, H/X) that have been published in criticality safety handbooks [1-5]. Curves are provided for highly-enriched uranium (HEU) and plutonium-239. Furthermore, the sensitivity of the effective neutron multiplication factor to changes in mass or cross-section data is plotted and discussed.

The results from MCNP-6.2 support the existing handbook curves relating critical mass to fissile concentration for metal-water mixtures. This behavior is shown in Figures 3 and 4 for ^{235}U and ^{239}Pu, respectively. From these plots, it is shown that MCNP-6.2 with ENDF/B-VII.1 data generally agree with the handbook curves [1,2,4,5] for ^{235}U to within +/- 5%, with certain regions differing by up to approximately +/- 10%. However, MCNP-6.2 does not agree as well with the curves for ^{239}Pu, with MCNP generally predicting smaller critical mass values than the handbook curves from [1,3] (there is good agreement with the curve from [2], which uses MCNP-4A calculations with ENDF/B-V nuclear data and was published in 1996).

The incremental reactivity worth of incremental additions of HEU or ^{239}Pu is provided with error bars in Figure 5. This plot can be used to relate margin in USL to margin in mass limits at various concentrations. For example, at 0.1 g/cc each additional gram of HEU or ^{239}Pu increases k_{eff} by approximately 0.028 and, a USL of 0.95 would imply a margin of approximately 175 g relative to a k_{eff} of 1.0. Figure 5 also shows that incremental mass changes in ^{239}Pu are more reactive than HEU at very high (metal) and very low (<0.3 g/cm^3) concentrations near criticality.

Curves calculated for subcritical limits are also presented in Figure 6 and discussed. These subcritical curves have a similar shape to the critical curves presented in Figures 3 and 4 but have critical mass values reduced by a greater percentage than the percent reduction in multiplication factor (e.g., a reduction in k_{eff} from 1.00 to 0.95 results in a critical mass decrease of much greater than 5%).

Lastly, the sensitivity of k_{eff} to perturbations in fission cross-section data is quantified and plotted for HEU and ^{239}Pu systems in Figures 7-10. These plots help to characterize the systems, provide a basis for comparison to other applications, and identify regions of increased importance in the underlying nuclear data.

KEY WORDS

Critical Mass Curve, MCNP Monte Carlo, Sensitivity

1. INTRODUCTION

Several published handbooks provide guidance about the quantities and geometries of fissionable material that may result in an inadvertent criticality. The critical mass limits of HEU and ^{239}Pu as reflected metal-water mixtures are two such examples. The curves for these limits are well-characterized and do not normally require further validation. This paper examines these curves, which are normally formed by using available experimental data, and compares them to curves generated with the Monte Carlo code MCNP-6.2 with ENDF/B-VII.1 nuclear cross-section data.

After a comparison of the MCNP-6.2-generated curves with the handbook curves, the MCNP-6.2 curves themselves will be analyzed to determine underlying sensitivity to cross-section data with respect to energy and fissile isotope concentration. The curves will also be analyzed to determine the reactivity worth of additional fissile mass versus concentration, and new mass curves with additional margin from the critical curves will be presented.

2. METHODOLOGY

Existing handbook curves were copied from several references [1-5] and several underlying data points were extracted to plot on the same axes as curves derived from MCNP-6.2 results. Other references were considered but were not included if the provided plots appeared to be duplicated in other references used in this study. The extracted plots for [1,3] were verified to agree with the values produced by CritView-1.02 [6]. The selected handbook curves relate the critical mass of ^{235}U (normally at 93.2 w/o [1]) and ^{239}Pu to concentration of the fissile nuclide in a solution or an idealized, homogenous metal-water mixture. The curves generated in this study use MCNP models with a very thick (30.48 cm) water reflector.

MCNP inputs were created and executed using a python script that interprets user-input and MCNP output values to modify a user-provided WORM input file [7]. The python script has the capability to modify any number of parameters as prescribed by the user and perform a parameter search on any other parameter. A simplified description of the process used for this study is documented as four general steps:

1. The python script initializes WORM, which creates three MCNP input decks, corresponding to the user-provided initial critical mass guess, the initial guess plus a user-defined uncertainty, and the initial guess minus a user-defined uncertainty at the first fissile concentration value of interest.
2. The initial three MCNP decks are executed, the results recorded in a log file, and the python script performs a linear interpolation/extrapolation of the mass corresponding to the desired k_{eff} value (1.0 in the baseline case) using the two points closest to the desired k_{eff} value.
3. The python script creates and executes WORM and MCNP files corresponding to the interpolated/extrapolated mass and compares the results to the desired k_{eff} value. The interpolation/extrapolation process is repeated until the MCNP result satisfies the convergence criterion. The baseline convergence criterion is +/-50 pcm (i.e., $0.99950 \leq k_{eff} \leq 1.00050$). The python script also increases/decreases the number of MCNP cycles (neutron generations) requested depending on the proximity of the previous iteration's results to the desired k_{eff} value so that better statistics are formed as the desired solution is approached.
4. Once the convergence is reached for the initial fissile concentration, the python script incrementally modifies the concentration value using WORM and uses the previous critical mass result for an initial guess at a new concentration. Steps 1-3 are followed at this new concentration until convergence is reached and the concentration is incrementally evaluated again, until the requested curve is completed.

The history of this process for the first six concentrations evaluated for the ^{235}U critical mass curve is provided in Table I. A graphical representation of steps 1-3, showing the first four linear interpolation/extrapolation predictions/results, is provided as Figure 1 for the first evaluated concentration of ^{235}U (15 g/L or H/X = 1763), while Figure 2 provides plots of mass and k_{eff} for each MCNP case comprising the first ten concentrations evaluated for ^{235}U.

Table I. Excerpt of history of search process for ^{235}U mass curve

15 g/L				15.736 g/L				16.508 g/L			
Case No.	Mass (g)	k_{eff}	σ	Case No.	Mass (g)	k_{eff}	σ	Case No.	Mass (g)	k_{eff}	σ
1	2263	0.9223	0.0004	11	6284	1.0179	0.0004	17	4632	1.0163	0.0003
2	2310	0.9242	0.0004	12	6479	1.0200	0.0003	18	4775	1.0185	0.0004
3	2356	0.9260	0.0004	13	6673	1.0205	0.0003	19	4918	1.0194	0.0004
4	4224	0.9729	0.0003	14	4608	0.9971	0.0003	20	3573	0.9970	0.0004
5	5306	0.9881	0.0004	15	4839	1.0011	0.0003	**21**	**3740**	**0.9996**	**0.0003**
6	6155	0.9952	0.0004	**16**	**4775**	**0.9996**	**0.0002**				
7	6719	1.0018	0.0002								
8	6564	1.0009	0.0002								
9	6410	0.9993	0.0002								
10	**6479**	**0.9998**	**0.0002**								

17.319 g/L				18.169 g/L				19.060 g/L			
Case No.	Mass (g)	k_{eff}	σ	Case No.	Mass (g)	k_{eff}	σ	Case No.	Mass (g)	k_{eff}	σ
22	3628	1.0141	0.0004	28	2970	1.0130	0.0004	32	2492	1.0109	0.0004
23	3740	1.0175	0.0004	29	3062	1.0159	0.0004	33	2569	1.0156	0.0004
24	3852	1.0191	0.0004	30	3154	1.0182	0.0004	34	2646	1.0184	0.0004
25	3166	1.0033	0.0004	**31**	**2569**	**0.9997**	**0.0004**	35	2315	1.0035	0.0004
26	3024	0.9988	0.0003					36	2229	1.0009	0.0003
27	**3062**	**0.9997**	**0.0002**					37	2202	0.9987	0.0002
								38	2218	0.9990	0.0003
								39	**2224**	**0.9996**	**0.0002**

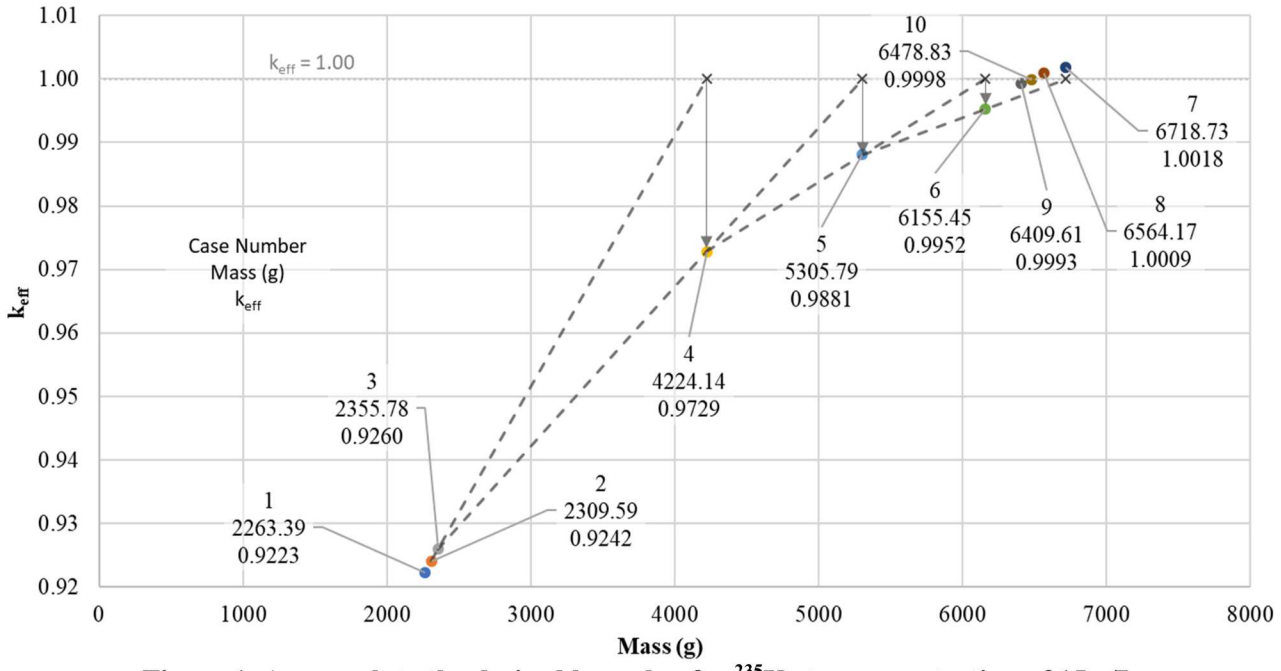

Figure 1. Approach to the desired k_{eff} value for ^{235}U at a concentration of 15 g/L

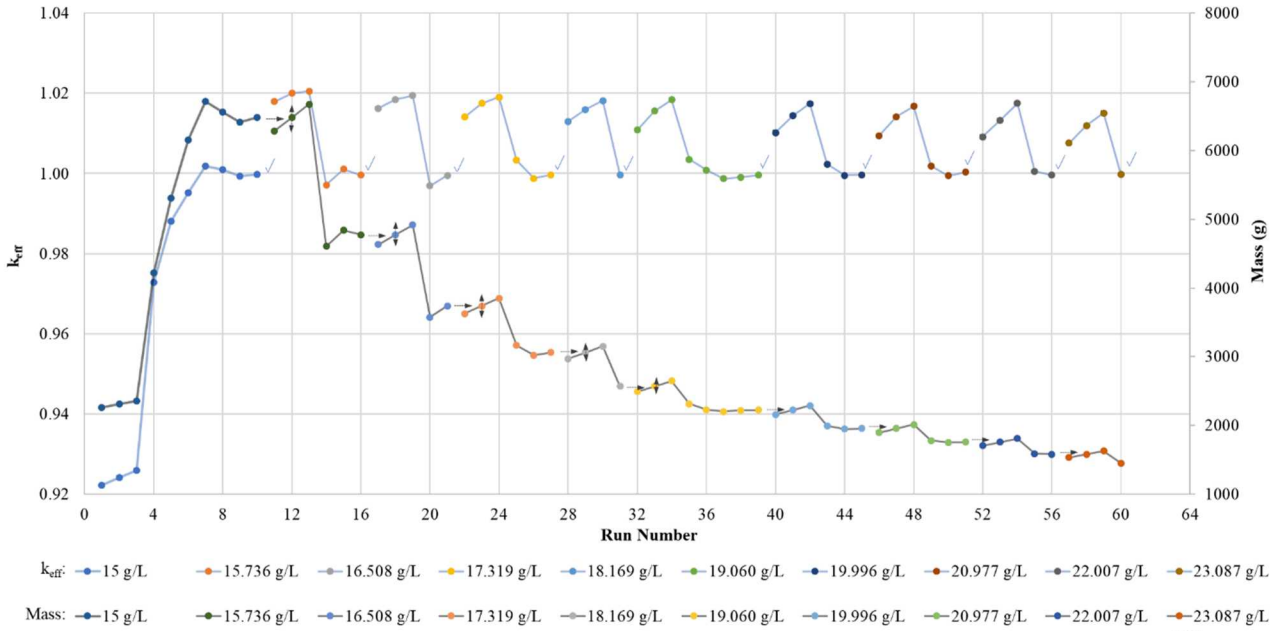

Figure 2. Convergence of k_{eff} and corresponding fissile mass for first 10 concentrations of ^{235}U

This analysis uses MCNP-6.2 with ENDF/B-VII.1 cross-section data.

3. RESULTS AND ANALYSIS

a. Baseline Critical Mass Curves

This section presents a comparison of the critical mass curves generated using MCNP with those from various criticality safety handbooks or guides [1-5].

Figure 3 provides a comparison of MCNP-generated results for ^{235}U critical mass to values taken from the handbooks. The values from [2] were generated using MCNP but were published in 1996. Reference [5] did not contain a curve but did contain tabulated points from experimental measurements; these points are plotted alongside the handbook curves. The percent differences in results from MCNP and the values from [1] and [2] are plotted on the secondary (right-side) vertical axis. Percent differences in results from MCNP to [4] are not plotted due to the curve being a subcritical curve and therefore resulting in a larger magnitude of the difference relative to the other reference values. The values from [4] reflect an additional margin of subcriticality, which causes them to be significantly (~30%) lower than the MCNP-generated critical results.

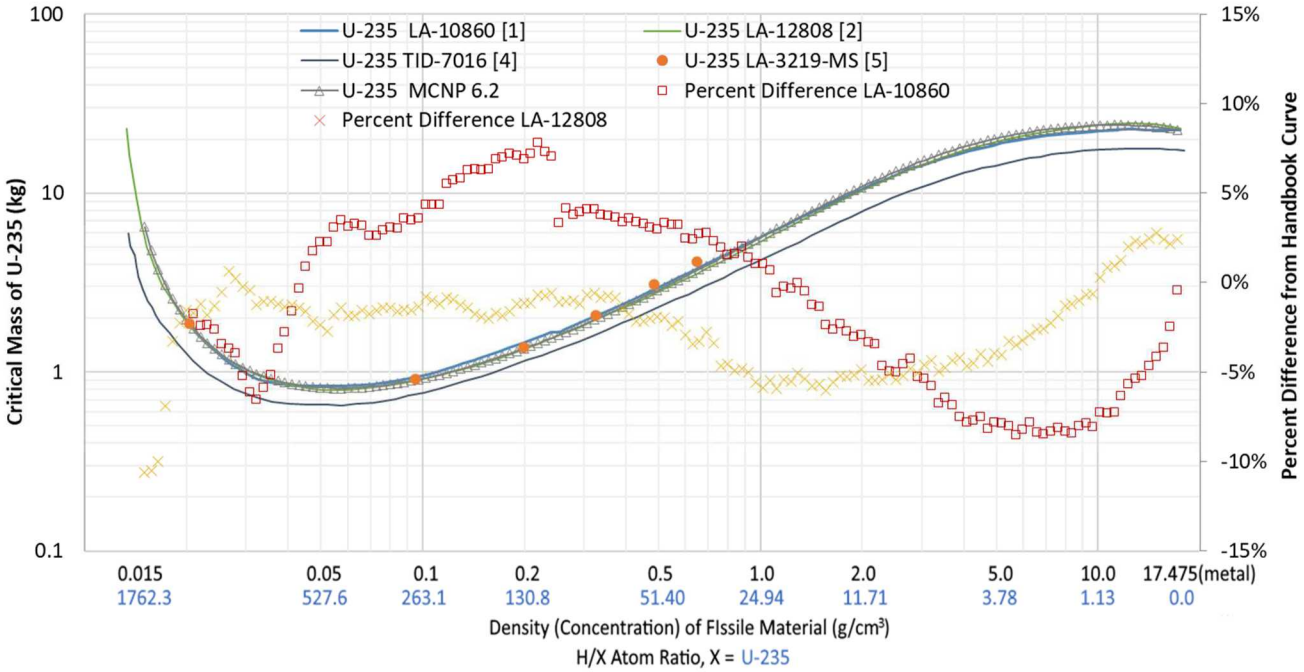

Figure 3. Comparison of MCNP-calculated ^{235}U critical mass with handbook correlations as a function of ^{235}U concentration

The results from Figure 3 demonstrate relatively good agreement between the handbook values and MCNP-calculated values. The values from [1] are generally within 8% of the MCNP values, while the values from [2] are generally within 5%. The MCNP-calculated critical mass limits are slightly above the values from [1] in the over-moderated and fast/metal regions of Figure 3 but are slightly below the values from [1] in the slightly under-moderated region. The MCNP-6.2-calculated critical mass limits are slightly above the values from [2] in the region from ~0.5 g/cm^3 to ~8 g/cm^3 (H/X of ~2 to ~50) but are otherwise in good agreement (while both sets were generated using MCNP, a different software version and different nuclear data was used).

Figure 4 is the ^{239}Pu analogue of Figure 3, with data taken from an additional handbook curve [3].

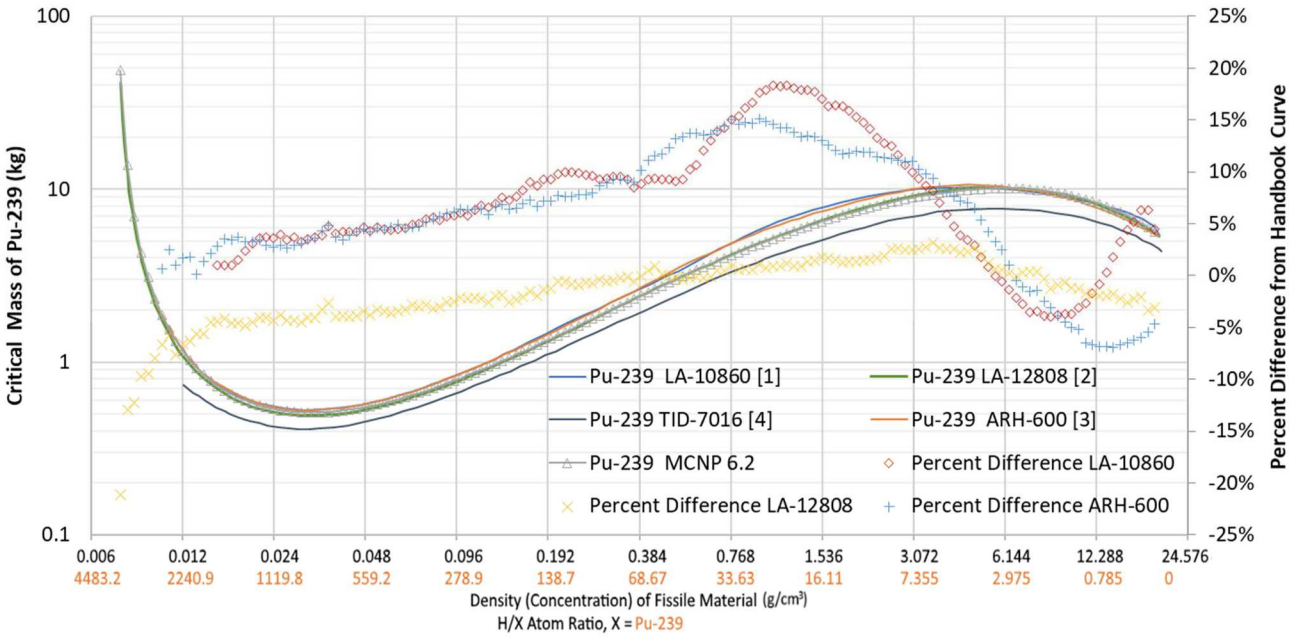

Figure 4. Comparison of MCNP-calculated ^{239}Pu critical mass with handbook correlations as a function of ^{239}Pu concentration

The results from Figure 4 show generally less agreement between MCNP values and handbook values for ^{239}Pu critical mass, especially in the under-moderated or epithermal energy range. This is consistent with the results and analysis documented in [8], which states that the difference in the results may be caused by the use of experimental data for PuO_2-polystyrene systems in that concentration range instead of the idealized, homogenous metal-water mixtures modelled in MCNP. The MCNP-supported critical mass values are closer to the values of [2] than [1] and [3] because [2] uses MCNP calculations (published in 1996), while the other references use experimental data. The values from [4] are again significantly lower than the MCNP-supported values due to the additional margin of subcriticality used in this handbook.

b. Sensitivity of k_{eff} to Variation in Mass

As can be expected, increases in fissile mixture mass at a given concentration result in increases to k_{eff}. This relationship can be of importance to understand how possible mass upsets to criticality limits affect system reactivity or how incorporating uncertainty into an upper subcritical limit (USL) for k_{eff} affects mass limits.

Using the iterative search data produced during the creation of the critical mass curves, estimates of sensitivity of k_{eff} to variations in the mass can be produced. Using the two MCNP runs closest to the desired k_{eff} value of 1.0 (notated as $n-1$ for the nearly converged case and n for the converged case), values for sensitivity and sensitivity uncertainty can be produced using Eqs. 1 and 2 respectively, where k and σ are the neutron multiplication eigenvalue and uncertainty value obtained from an MCNP run and m is the corresponding input fissile isotope mass.

$$S_m \left[\frac{\Delta k}{g}\right] = \frac{k_{n-1}-k_n}{m_{n-1}-m_n} \approx \frac{\partial k}{\partial m} \tag{1}$$

$$\sigma_{S_m} \left[\frac{\Delta k}{g}\right] = \frac{\sqrt{\sigma_{n-1}^2+\sigma_n^2}}{|m_{n-1}-m_n|} \tag{2}$$

The values obtained from using Eqs. 1 and 2 are plotted for HEU and ^{239}Pu in Figure 5. This plot shows a similar trend for both HEU (represented by blue diamonds in Figure 5) and ^{239}Pu (orange triangles), but with ^{239}Pu being more reactive per unit mass at dilute or very-well-moderated and nearly metal concentrations (both ends of the plot). These trends have similar shapes to the average reactivity per unit mass calculated directly from the critical mass curves provided in Figures 3 and 4 (plotted in Figure 5 as gray squares and yellow crosses for HEU and ^{239}Pu, respectively), but are reduced by a factor of about 3 to 5. From this reduction, it is understood that additional increments of mass have decreasing reactivity worth, consistent with decreasing returns on incremental mass additions to spherical volume and neutron leakage.

Oftentimes, sensitivity values are reported as normalized, unitless values. To normalize the values from Figure 5, one can simply divide the plotted sensitivity values by the average worth values obtained from the critical mass curves to obtain a formulation of $(\Delta k/k)/(\Delta m/m)$. Doing this yields a normalized sensitivity value that is generally between 0.18 and 0.43, with an average value between 0.28 and 0.29 for both HEU and ^{239}Pu. Thus, it is expected that a 1% change in mass for these systems that are approximately critical will result in a 0.18-0.43% change in k_{eff}, with an approximate average change between 0.28% and 0.29%.

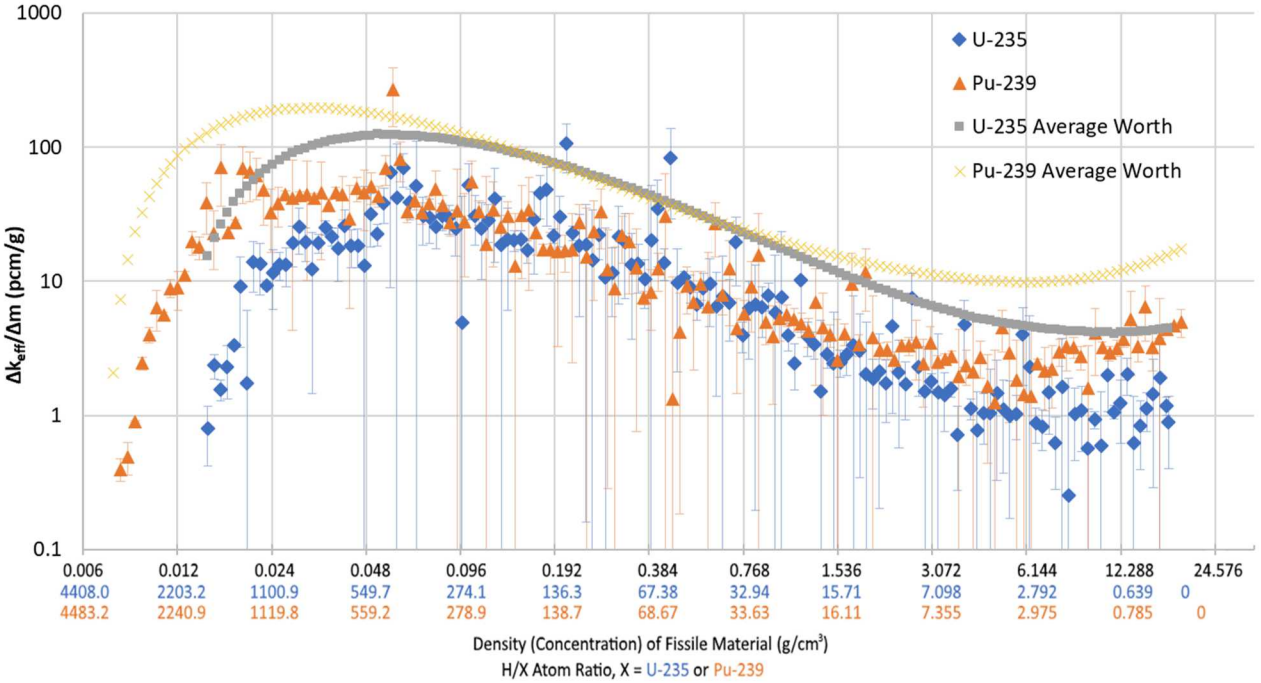

Figure 5. Sensitivity of k_{eff} to mass near criticality and average reactivity worth per unit mass for HEU and ^{239}Pu

Another way to visualize the sensitivity of k_{eff} to mass is to plot mass values at various values of k_{eff} other than 1.0 (i.e., characterize the sensitivity of mass to a desired k_{eff}). The critical mass curves for k_{eff} of 0.95 and 0.90 are plotted alongside the critical mass curve for ^{235}U in Figure 6. The MCNP-generated handbook curves from [2] for k_{eff} of 1.0 and 0.90 are also plotted in Figure 6 for reference and comparison.

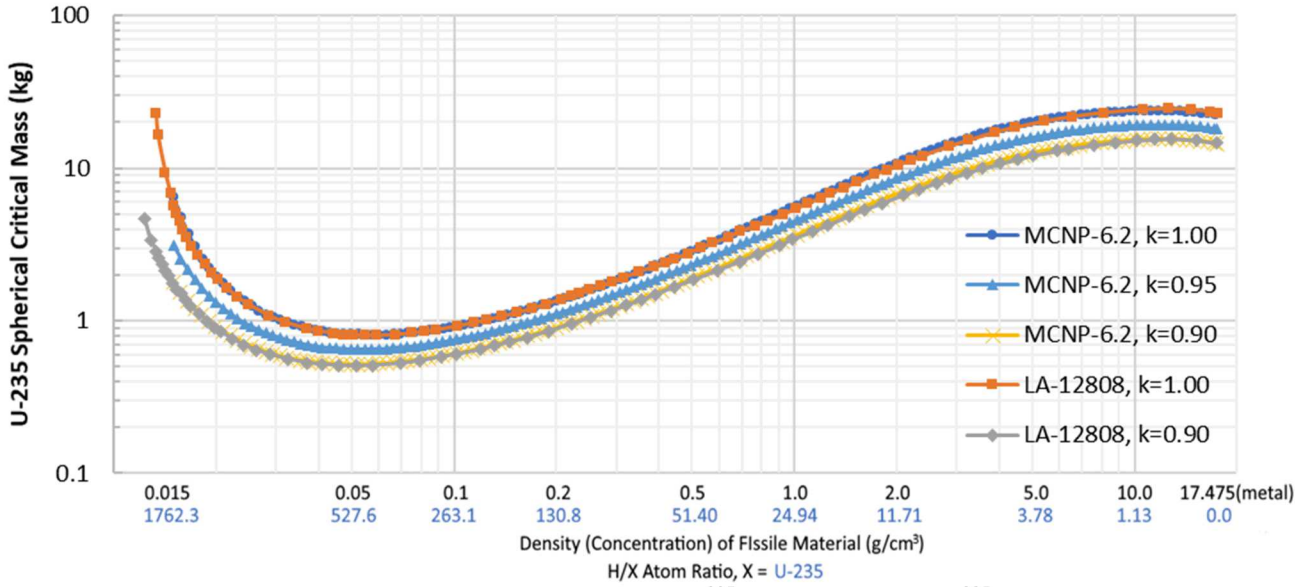

Figure 6. Critical and subcritical mass curves for ^{235}U as a function of ^{235}U concentration

The results shown in Figure 6 for k_{eff} of 0.95 and 0.90 are consistent with the curve from [2] and the sensitivity analysis performed earlier in this section, with the curves maintaining a similar shape on a log-log plot, and a reduction in k_{eff} of 10% resulting in a reduction of ~40% of the corresponding mass.

c. Sensitivity of k_{eff} to Variation in Fission Cross Section Data

The sensitivity of k_{eff} to changes in nuclear cross-section data may be used to demonstrate correlation between computational models and experiments. Because of the simplicity of the models used in this study and the breadth of knowledge associated with the critical mass curves for ^{235}U and ^{239}Pu, this sensitivity analysis may be useful to apply here.

Figure 7 provides a three-dimensional surface plot of the sensitivity per unit lethargy of k_{eff} to changes in the ^{235}U fission cross-section, $(\Delta k/k)/(\Delta\sigma_{235,f}/\sigma_{235,f})$, across 44 energy groups for critical metal/water systems as a function of ^{235}U concentration. Figure 8 provides the same data as a 2-D contour plot with the energy corresponding to the average neutron lethargy causing fission (EALF) from the MCNP results for each ^{235}U concentration overlaid. These plots illustrate the large sensitivity of unmoderated systems to fission cross-section at large energies (near the Watt fission energy spectrum range) and of well-moderated systems to fission cross-section at thermal energies. Furthermore, sensitivity to cross-section data in the resonance region is considerable, especially for ^{235}U concentrations of roughly 700-4000 g/L (epithermal or poorly moderated systems). The EALF parameter is consistent with the sensitivity to the fission cross-section and may be considered a good indication of neutron spectrum hardness and behavior for certain applications. It is expected that these sensitivity plots would change, especially in the resonance energy range, if uranium enrichment were to be modified, as neutron capture from the resonances in ^{238}U cross-sections would change the energy-dependent flux available for ^{235}U fission. This study uses an enrichment of 93.2% [1].

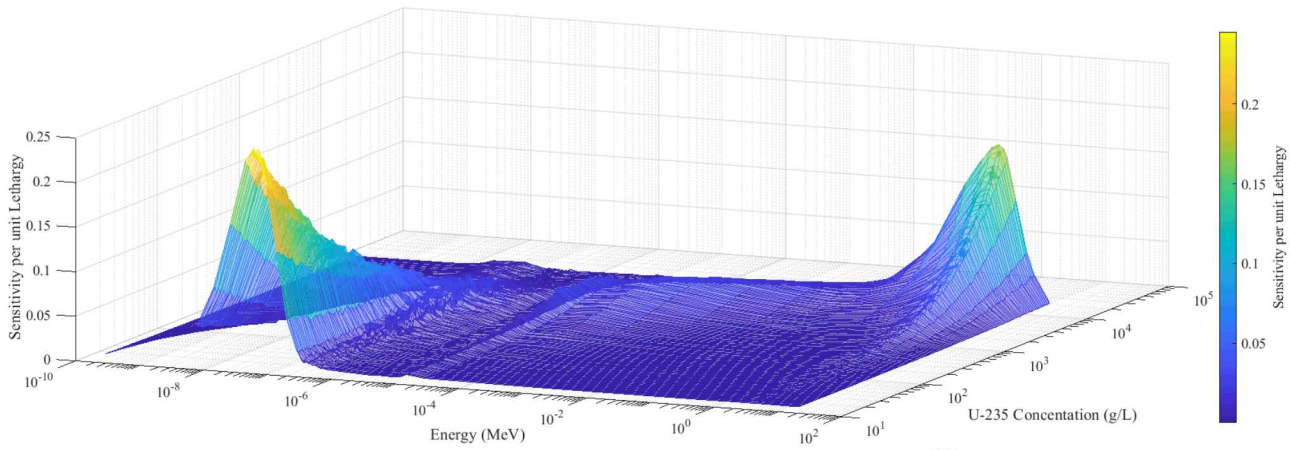

Figure 7. Sensitivity of k_{eff} per unit lethargy to the fission cross-section of ^{235}U as a function of energy and concentration of ^{235}U in a metal-water mixture

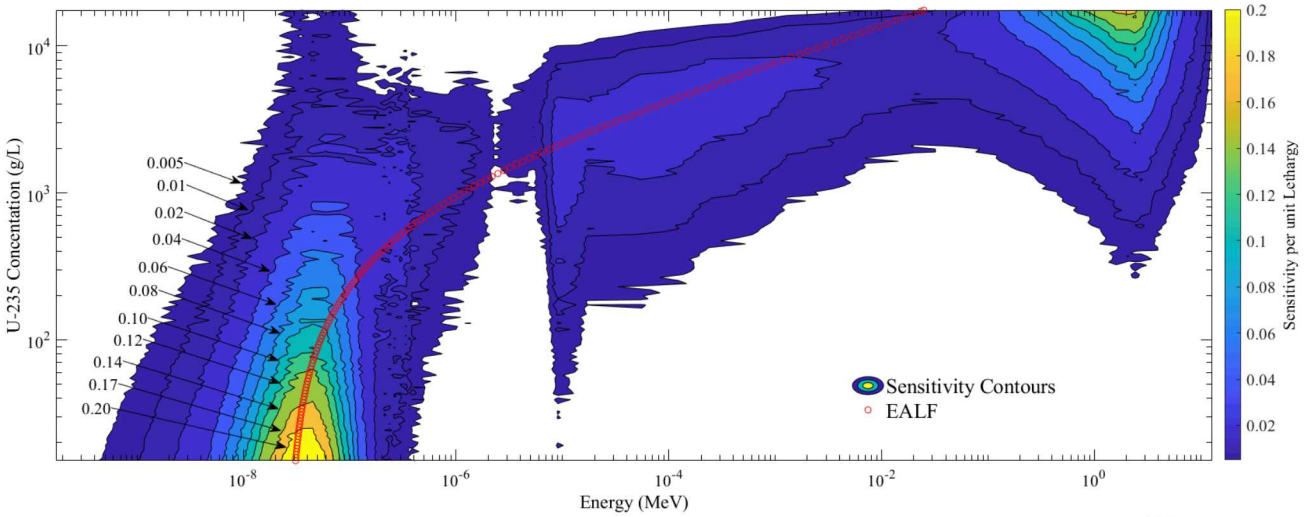

Figure 8. Contour plot of sensitivity of k_{eff} per unit lethargy to the fission cross-section of ^{235}U with EALF plotted in the energy-concentration plane

Figures 9 and 10 are the ^{239}Pu analogues of Figures 7 and 8. The ^{239}Pu plots differ from their ^{235}U counterparts in several ways. Several of these differences are the result of differing behavior from the two different nuclides. In general, ^{239}Pu has larger sensitivity values than ^{235}U, especially in the fast (fission-spectrum) energy range. This may be due to the larger (by about 30-50%) fast fission cross-section for ^{239}Pu and the greater number of neutrons generated per fission ($\bar{\nu}$) in ^{239}Pu (at all energies) relative to ^{235}U. Another feature evident in Figures 9 and 10 is the large sensitivity of k_{eff} to variations in the ^{239}Pu fission cross-section data in the 0.2-0.4 eV energy range; this increased sensitivity corresponds to a large, wide resonance in the ENDF/B-VII.1 cross-section data in the same energy range. For several ^{239}Pu concentrations (approximately 100 g/L – 2000 g/L), this resonance energy range exhibits the greatest sensitivity per unit lethargy across the entire energy spectrum.

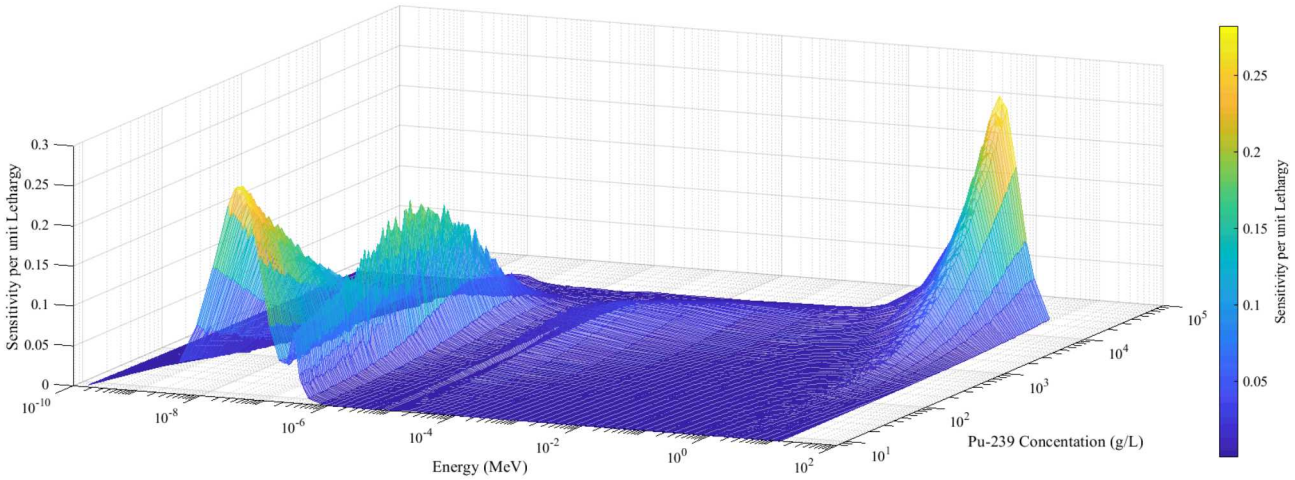

Figure 9. Sensitivity of k_{eff} per unit lethargy to the fission cross-section of ^{239}Pu as a function of energy and concentration of ^{239}Pu in a metal-water mixture

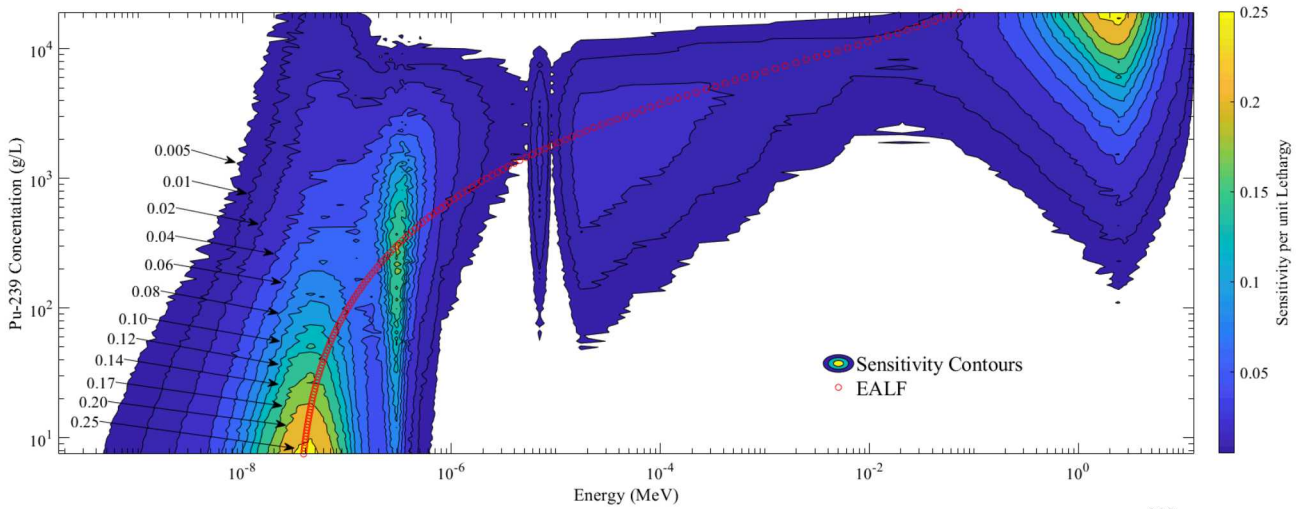

Figure 10. Contour plot of sensitivity of k_{eff} per unit lethargy to the fission cross-section of ^{239}Pu with EALF plotted in the energy-concentration plane

4. CONCLUSIONS

Results generated using MCNP-6.2 with ENDF/B-VII.1 are consistent with several handbook critical mass curves [1-5]. Further evaluation of these curves and the data used to generate them reveals that the reactivity worth of incremental unit of mass in systems that are critical or nearly critical is worth less than the average reactivity worth per unit of existing mass in the system. This also means that, in order to obtain a given margin in k_{eff} (e.g., 5% or a USL of 0.95), a greater reduction in the corresponding mass limit must be made (e.g., a ~25% reduction from the critical mass value). Furthermore, the sensitivity of k_{eff} to cross-section data for fission of the fissile isotope was quantified and plotted. These plots can be used to characterize the system for comparison or validation against other systems.

ACKNOWLEDGMENTS AND DISCLOSURE

Sandia National Laboratories is a multi-mission laboratory managed and operated by National Technology and Engineering Solutions of Sandia, LLC, a wholly owned subsidiary of Honeywell International, Inc., for the U.S. Department of Energy's National Nuclear Security Administration under contract DE-NA000352. This paper describes objective technical results and analysis. Any subjective views or opinions that might be expressed in the paper do not necessarily represent the views of the U.S. Department of Energy or the United States Government.

The research presented in this paper was supported by a U.S. Department of Energy Nuclear Safety Research and Development (NSR&D) Program-Funded Project. In addition to the NSR&D program, the authors would like to acknowledge the collaboration between those involved at Sandia National Laboratories, Los Alamos National Laboratory, and the University of New Mexico that helped to produce this work.

REFERENCES

[1] H. C. Paxton, N. L. Pruvost, *LA-10860-MS: Critical Dimensions of Systems Containing ^{235}U, ^{239}Pu, and ^{233}U*, Los Alamos National Laboratory (1987).

[2] N. L. Pruvost, H. C. Paxton (Ed.), *LA-12808: Nuclear Criticality Safety Guide*, Los Alamos National Laboratory (1996).

[3] R. D. Carter, G. R. Kiel, K. R. Ridgway, *ARH-600: Criticality Handbook Volume II*, Atlantic Richfield Hanford Company (1969).

[4] J. T. Thomas (Ed.), *TID-7016 Rev. 2: Nuclear Safety Guide (NUREG/CR-0095)*, Union Carbide Corporation (1978).

[5] C. B. Mills, *LA-3219-MS: Critical Assemblies of Fissionable Materials*, Los Alamos Scientific Laboratory of the University of California (1959).

[6] S. H. Finfrock, *CritView User's Guide*, CH2M Hill, (2009).

[7] T. Jones, "WORM: A General-Purpose Input Deck Specification Language," *Trans. Am. Nucl. Soc.*, **81**, pp.164-165 (1999).

[8] J. L. Alwin, N. Zhang, *LA-UR-16-27371: Plutonium Critical Mass Curve Comparison to Mass at Upper Subcritical Limit (USL) Using Whisper,* Los Alamos National Laboratory (2016).